

$^{12}\text{C} + ^{12}\text{C}$  transfer reactions at 93.8 MeV

C. B. Fulmer, R. M. Wieland, D. C. Hensley, S. Raman, G. R. Satchler, A. H. Snell, P. H. Stelson, and R. G. Stokstad

Oak Ridge National Laboratory, Oak Ridge, Tennessee 37830

(Received 6 June 1978)

Angular distributions of the most intense one- and two-nucleon transfer reactions induced by 93.8 MeV  $^{12}\text{C}$  ions on a  $^{12}\text{C}$  target were measured over the angular range 10–65°. The reactions are selective in that only a few of the available states are strongly excited. For both single proton and single neutron transfer,  $p_{1/2}$  and  $d_{5/2}$  shells are populated with about equal probability; for  $pn$  transfer the strongest peak corresponds to the  $5^+$  level of  $^{14}\text{N}$ . The sum of the cross sections for all of these transfer reactions, integrated over the measured angular range, is 7.5 mb. This may be compared with 23 mb for the inelastic scattering to the  $2^+$  level of  $^{12}\text{C}$  and 7 mb for mutual excitation of the  $2^+$  level in the target and projectile. Distorted-wave Born-approximation calculations are compared with the measured angular distributions for a number of the transfer reactions.

[NUCLEAR REACTIONS  $^{12}\text{C}(^{12}\text{C}, ^{11}\text{C})$ ,  $^{12}\text{C}(^{12}\text{C}, ^{11}\text{B})$ ,  $^{12}\text{C}(^{12}\text{C}, ^{10}\text{B})$   $E = 93.8$  MeV; ]  
measured  $\sigma(\theta)$ ; DWBA analyses.

## INTRODUCTION

Early experimental studies of heavy-ion-induced transfer reactions both at very low energies<sup>1,2</sup> and at energies far above the Coulomb barrier<sup>3-5</sup> found a pronounced selectivity in the population of the final states and featureless exponential angular distributions. This selectivity is apparently a general characteristic of these reactions, whereas featureless angular distributions are not. For Coulomb dominated transfer reactions<sup>6</sup> induced by medium heavy ions, angular distributions are characterized by smooth bell-shaped peaks (near the grazing angle) with oscillations superimposed as the incident particle energy is increased.<sup>7-9</sup> Measurements at very forward angles<sup>10,11</sup> showed a diffraction-like structure in the forward-angle region even at energies where a smooth bell-shaped angular distribution is observed in the grazing angle region.

Theoretical interpretations ranging from semiclassical descriptions to distorted-wave Born approximation (DWBA) analyses<sup>12</sup> have been applied to heavy-ion transfer reactions. At high incident energies projectiles such as  $^{12}\text{C}$  introduce an angular momentum in a grazing collision which usually exceeds the critical value that a compound nucleus (of the projectile and a light target) can support<sup>13,14</sup>; hence direct reactions dominate. Kinematic selection rules relating  $Q$  value and angular momentum transfer at energies well above the Coulomb barrier have been developed<sup>15</sup> which indicate reactions with large angular momentum transfer are favored.

In the work reported here, cross sections were

measured over a wide angular range for the most intense one- and two-nucleon transfer reactions induced by 93.8 MeV  $^{12}\text{C}$  ions on a  $^{12}\text{C}$  target. These measurements are part of an extensive study<sup>16-21</sup> of  $^{12}\text{C} + ^{12}\text{C}$  reactions in which elastic and inelastic angular distributions were measured at 14 laboratory energies over the range of 72.4 to 126.7 MeV. In these data inelastic scattering to the  $2^+$  (4.43 MeV) state of  $^{12}\text{C}$  was observed to be very intense; at angles beyond  $\sim 45^\circ$  c.m. both single and mutual excitations of the  $2^+$  level occur with cross sections larger than that of elastic scattering. This raises the question of whether single or multiple nucleon transfer might also be strong processes which could indirectly affect the elastic and inelastic scattering. Measurement of these processes would be important for a reaction model that includes the effect of "double transfer" on elastic and inelastic scattering. While many measurements of transfer reactions in this mass region have been reported, most of these covered smaller angular ranges, and only a few measurements<sup>22-24</sup> were made for the  $^{12}\text{C} + ^{12}\text{C}$  system.

## EXPERIMENTAL

A beam of  $^{12}\text{C}^{4+}$  ions from the Oak Ridge Isochronous Cyclotron was used for these measurements. The ions passed through a beam analyzing magnet (which determined the energy, 93.8 MeV), through a 75 cm diameter scattering chamber, and thence into a Faraday cup. At the entrance to the Faraday cup, a permanent magnet was used to prevent secondary electrons from entering or leaving the cup. A particle detector at a fixed

angle of  $10^\circ$  was used to monitor carbon buildup on the target and to enable us to correct for this effect.

The target was self-supporting natural carbon foil of thickness  $180 \mu\text{g}/\text{cm}^2$ . The thickness was determined by measuring the energy loss of 5.75 MeV  $\alpha$  particles in the target and in thicker foils which were weighed. Reaction products were detected in two  $\Delta E$ - $E$  semiconductor telescopes positioned 22.1 cm from the target. The  $\Delta E$  resolution was adequate to resolve neighboring isotopes of B, C, and N;  $E$  resolution was  $\sim 300$  keV. A collimator 0.158 cm wide and 0.953 cm high 15 cm ahead of the target defined the beam spot on the target. The defining apertures for the detector telescopes subtended angles of  $0.41^\circ$  in the scattering plane and azimuthal angles of  $1.80^\circ$ . Absolute cross sections were deduced from the measured target thickness, integrated beam current, and detector solid angles. The absolute normalization is estimated to have a probable error of  $\pm 13\%$ .

The data comprise fairly complete angular distributions for the more intense reactions rather than less extensive measurement on all the transfer reactions that could possibly be identified. Experimental data are available in tabular form in Ref. 20. Integrated beams ranged from  $\sim 40 \mu\text{C}$  at forward angles to  $\sim 400 \mu\text{C}$  at the largest angles.

#### EXPERIMENTAL RESULTS

Figure 1 shows an energy spectrum for the  $^{10}\text{B}$  reaction product. These data illustrate the selectivity of the reactions; there are few strong peaks in the spectrum even though a large number of excited states are available. The peak at 8.96 MeV

is evidently due to excitation of the 8.96 MeV,  $5^+$  level in  $^{14}\text{N}$ , and is the dominant peak in all of the  $^{10}\text{B}$  data.

In Fig. 2, elastic and inelastic angular distributions (also at 93.8 MeV incident particle energy) are compared with those for one- and two-nucleon ground-state transfer reactions. The  $2n$ ,  $2p$ , and  $p2n$  transfer reactions were also observed but with cross sections much smaller than those for the one-nucleon and  $pn$  transfer reactions.

Angular distributions for the strongest single nucleon transfer reactions are shown in Fig. 3. Proton transfer data for less prominent peaks at  $E^* = 2.25$  and 4.44 MeV are also shown. In most cases, these cross sections were obtained from separate measurements of each of the outgoing particles (e.g.,  $^{11}\text{C}$  and  $^{13}\text{C}$  for single nucleon transfer). The ground-state angular distributions for single nucleon transfer ( $n$  or  $p$ ) are very similar as would be expected on the basis of isospin symmetry; the  $Q$  values differ by only 0.24 MeV.

The measured cross sections for single nucleon transfer reactions were integrated over the range of the data ( $10^\circ$ - $65^\circ$ ). The values thus obtained are presented in Fig. 4. Energy levels of the two ejectiles for each case are also indicated on the same energy scale. Since all excited levels of  $^{13}\text{N}$  are unbound to particle emission, any peaks observed in the  $^{13}\text{N}$  energy spectra correspond simply to states in  $^{11}\text{B}$ . The cross sections obtained from the  $^{13}\text{N}$  spectra and from the  $^{11}\text{B}$  spectra for the 2.25 MeV proton transfer are about equal; and this transfer must, therefore, be principally due to excitation of the 2.12 MeV  $\frac{1}{2}^-$  level in  $^{11}\text{B}$ . We note that this level is excited with a cross section

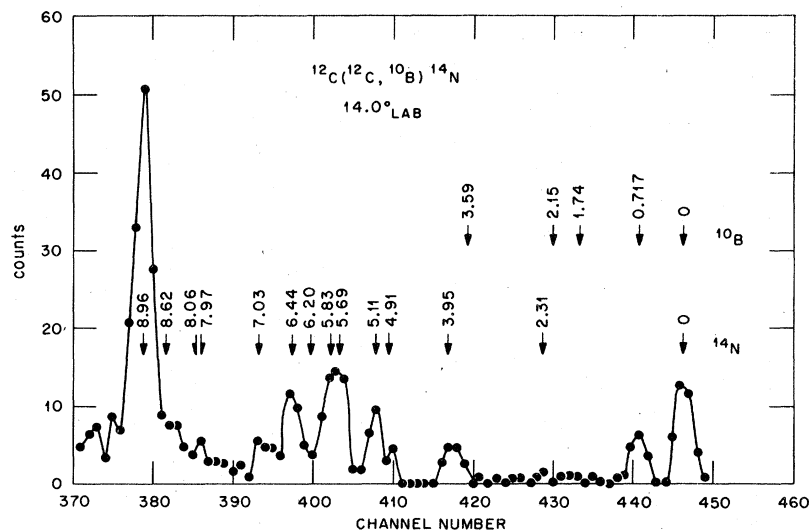


FIG. 1. Energy spectrum of  $^{10}\text{B}$  ions observed in the  $^{12}\text{C}(^{12}\text{C}, ^{10}\text{B})^{14}\text{N}$  reaction at  $E_{\text{lab}} = 93.8$  MeV. Excited states in  $^{14}\text{N}$  below 9 MeV and in  $^{10}\text{B}$  below 3.6 MeV are indicated by arrows to illustrate the selective nature of the reaction.

comparable to that for the  $\frac{1}{2}^-$  level at 2.0 MeV in  $^{11}\text{C}$  (from neutron transfer). A dashed line indicates the estimated cross section for exciting the 4.31 MeV  $\frac{5}{2}^-$  level in  $^{11}\text{C}$ ; the uncertainty is  $\sim 50\%$ .

Figure 5 presents angular distributions for the peaks observed in the  $np$  transfer reactions. For

most of these reactions, the decrease of the cross section with increasing angle is less rapid than that for the one-nucleon transfer reactions. The integrated cross sections ( $10^\circ \leq \theta \leq 65^\circ$ ) are shown in Fig. 6 with energy levels of the ejectiles plotted on the same energy scale. Since in heavy-ion

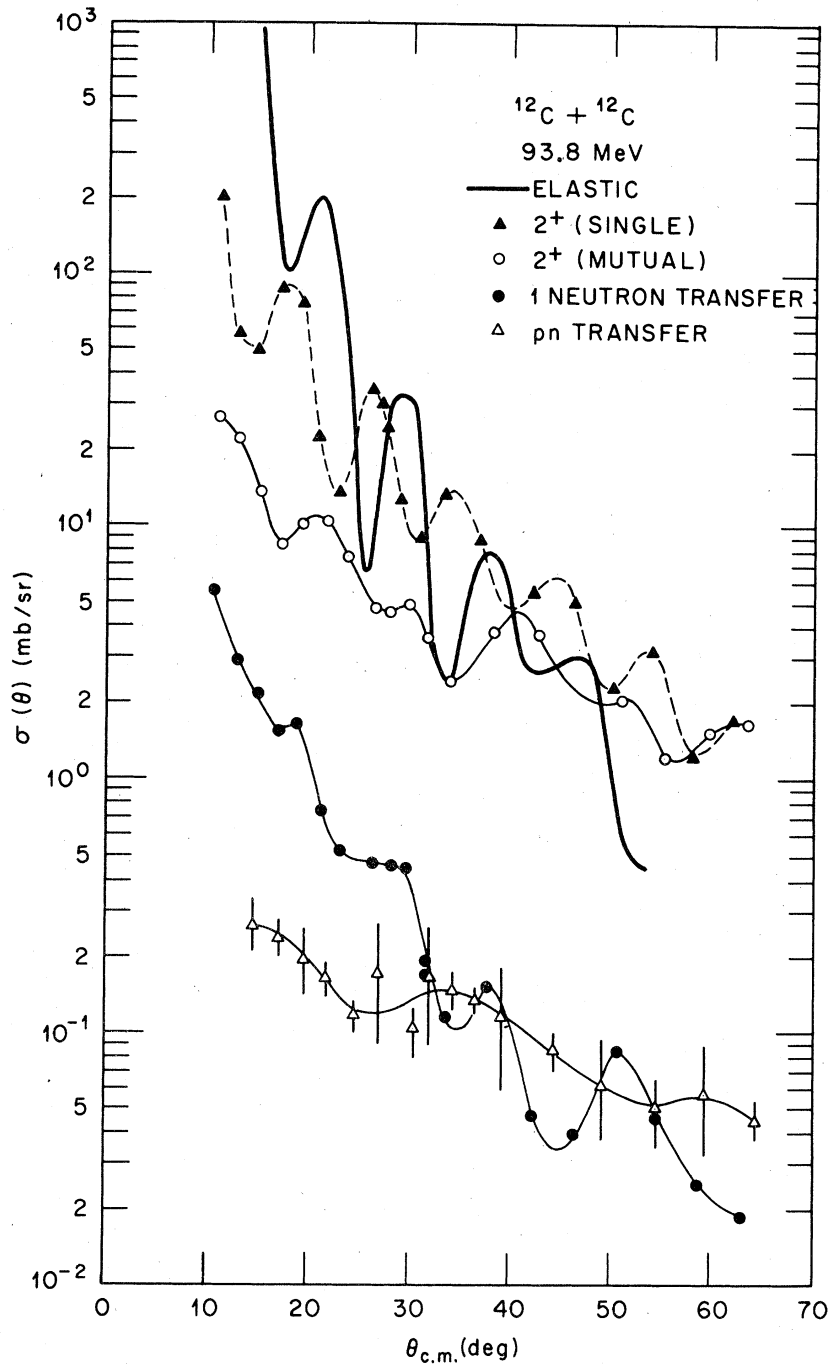


FIG. 2. A comparison of the measured angular distributions for elastic and inelastic scattering and for representative transfer reactions at 93.8 MeV. The two particle transfer data shown are for the ground-state reactions. The curves are drawn to guide the eye.

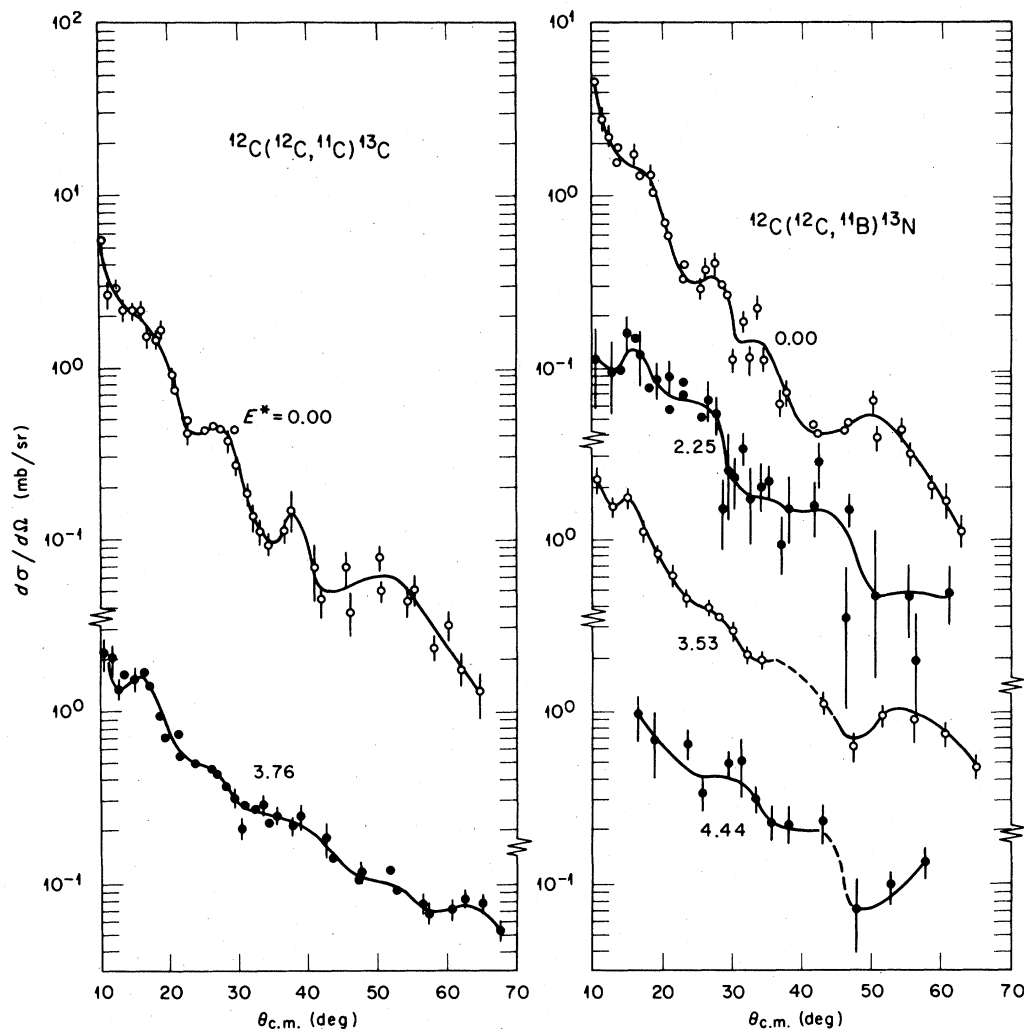


FIG. 3. Measured angular distributions for  $^{12}\text{C} + ^{12}\text{C}$  nucleon transfer reactions at 93.8 MeV. The curves are drawn to guide the eye.

transfer reactions both ejectiles may be in excited states, we have also plotted the  $^{14}\text{N}$  energy levels on a scale corresponding to mutual excitation of the  $^{10}\text{B}$   $1^+$  level at 0.72 MeV. The yield observed at  $E^* = 9.68$  MeV may arise principally from mutual excitation of the 8.96 MeV level in  $^{14}\text{N}$  and the 0.72 MeV level in  $^{10}\text{B}$ . Similarly the yield observed at  $E^* = 7.0$  MeV may include a contribution from mutual excitation of the 6.44 MeV level in  $^{14}\text{N}$  and the 0.72 MeV in  $^{10}\text{B}$   $1^+$  (see Fig. 1).

#### DISCUSSION

Because of the symmetry about  $90^\circ$  c.m. for the  $^{12}\text{C} + ^{12}\text{C}$  reaction,<sup>25</sup> the data presented above constitute rather complete angular distributions. The initial motivation for these measurements was to

obtain data for the most intense transfer reactions and to use the results to calculate the effect of "double transfer" contributions to elastic and inelastic scattering.<sup>26</sup> We see in Fig. 2 that over the range of the data these transfer reactions occur with appreciably smaller cross sections than those for either elastic scattering or inelastic scattering to the  $2^+$  level. In Table I, we compare the integrated cross sections ( $10^\circ \leq \theta \leq 65^\circ$ ) for several reactions. The transfer reactions include all excited states for which angular distributions were obtained. While the data for single nucleon transfer include only those levels below 5 MeV, we believe these are the most intense ones; the data at higher excitation exhibited no strong peaks. In the Oxford measurements at 114 MeV incident particle energy,<sup>23,24</sup> the energy spectra for single nucleon transfer extend to  $E^* \sim 16$  MeV but show no

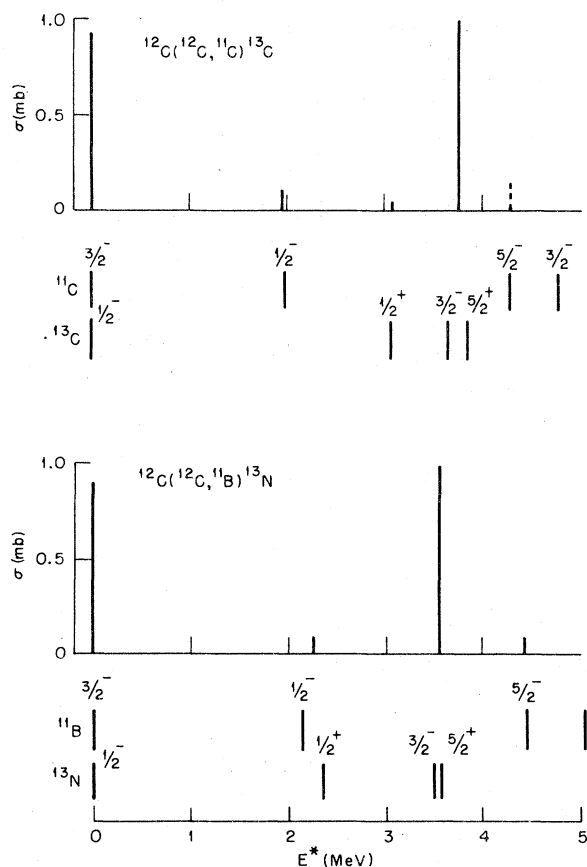


FIG. 4. Measured cross sections for single nucleon transfer reactions for  $^{12}\text{C} + ^{12}\text{C}$  at 93.8 MeV, where  $\sigma = 2\pi \int_{10}^{60} \sin\theta \sigma(\theta) d\theta$ .

strong peaks above the  $\frac{5}{2}^+$  levels of the  $A = 13$  reaction products.

In a stripping reaction on a  $^{12}\text{C}$  target nucleons may be transferred into either the  $p$  or ( $sd$ ) shells. Since the  $p_{3/2}$  shell in  $^{12}\text{C}$  is  $\sim 80\%$  filled,<sup>20</sup> the transfer to  $p_{1/2}$  should be stronger than to  $p_{3/2}$ . Note in Fig. 4 that the  $\frac{1}{2}^-$  ground states and the  $\frac{5}{2}^+$  levels of the mass 13 reaction products are the levels principally excited in both the neutron and proton transfer reactions. The pronounced similarity of neutron and proton transfer reactions is apparent both in the levels excited (Fig. 4) and in the summed integrated cross sections (Table I).

The energy resolution was inadequate to separate the  $\frac{5}{2}^+$  particle states of  $^{13}\text{C}$  and  $^{13}\text{N}$  from the respective nearby  $\frac{3}{2}^-$  hole states. Inasmuch as the hole states are generally weakly excited in stripping reactions on  $^{12}\text{C}$ , the yields shown in Fig. 4 at  $\sim 3.7$  MeV, are believed to arise principally from excitation of the  $\frac{5}{2}^+$  states. The  $\frac{3}{2}^-$  and  $\frac{5}{2}^+$  levels of  $^{13}\text{C}$  were resolved in high resolution measurements of neutron stripping on a  $^{12}\text{C}$  target

with  $^7\text{Li}$  ions,<sup>27</sup> and the yield of  $\frac{3}{2}^-$  was an order of magnitude smaller than that of  $\frac{5}{2}^+$ .

In a number of transfer reactions on  $^{12}\text{C}$  largely structureless angular distributions that decrease exponentially with angle have been observed. Incident projectiles included  $^{11}\text{B}$  at 115 MeV and  $^{10}\text{B}$  at 105 MeV (Ref. 3),  $^{14}\text{N}$  at 78 MeV (Ref. 28), at 148 MeV (Ref. 4), at 155 MeV (Ref. 29); and  $^{12}\text{C}$  at 114 MeV (Ref. 23). This lack of structure has been attributed to recoil effects<sup>30</sup> for a number of cases for which excellent agreement using exact-recoil DWBA calculations was obtained.<sup>31,32</sup> The almost featureless behavior of the angular distributions for 155 MeV  $^{14}\text{N}$  (Ref. 29) was attributed to effects of the absorptive part of the nuclear optical potential.

The diffraction-like oscillations, while not large, are clearly apparent in most of the angular distributions measured in the present work. This is in contrast with the transfer reactions on  $^{12}\text{C}$  for a variety of incident projectiles cited above. In Fig. 7 angular distributions for a single nucleon transfer and an  $np$  transfer reaction induced by 93.8 MeV  $^{12}\text{C}$  (present work) and by 114 MeV  $^{11}\text{B}$  (Ref. 3) are contrasted. There is considerable similarity in the shape of the angular distributions for the one-proton transfer, but for the  $pn$  transfer angular distributions, there are significant differences, both in structure and slope, between the  $^{12}\text{C}$  and  $^{11}\text{B}$  data.

As was noted above the ground state  $\frac{1}{2}^-$  and the  $\frac{5}{2}^+$  levels of the mass 13 reaction products are the levels most strongly excited in the present single nucleon transfer reactions. The integrated yields (Fig. 4) for these two levels are about equal for both neutron and proton transfer; this is true also for the 114 MeV  $^{12}\text{C} + ^{12}\text{C}$  data reported in Ref. 24. In contrast to this a marked preference for exciting the  $\frac{5}{2}^+$  level has been observed for the following projectiles on  $^{12}\text{C}$  targets:  $^{11}\text{B}$  at 115 MeV (Ref. 3),  $^{16}\text{O}$  at 128 MeV (Ref. 24),  $^{14}\text{N}$  at 78 MeV, and 155 MeV (Ref. 29), at 100 MeV (Ref. 33) and at 148 MeV (Ref. 4).

Relative cross sections were calculated in Ref. 23 with a semiclassical model in which it was assumed that transfers take place near the nuclear surface, when the projectile and target undergo a grazing collision. This model assumes a dependence of cross sections on bombarding energy,  $Q$  value of the reaction, and  $J_1$  and  $J_2$  of the transferred nucleon. The calculations indicate, in fact, less preference for exciting the  $\frac{5}{2}^+$  states relative to the ground states if the incident projectile is  $^{12}\text{C}$  rather than  $^{11}\text{B}$ ,  $^{14}\text{N}$ , or  $^{16}\text{O}$ .

The semiclassical model has also been used (Ref. 23) to calculate relative cross sections for a number of multiple nucleon transfer reactions,

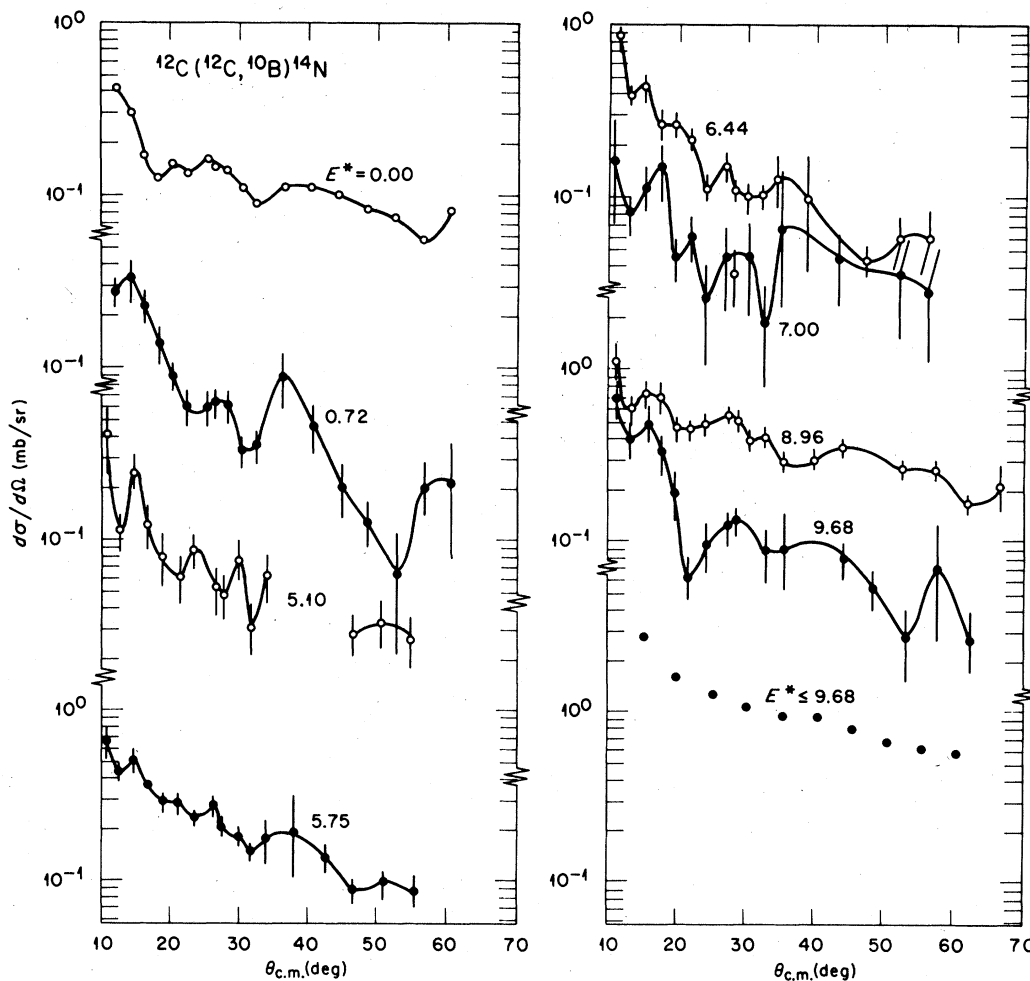


FIG. 5. Measured angular distributions for  $^{12}\text{C} + ^{12}\text{C}$   $np$  transfer reactions at 93.8 MeV. The curves are drawn to guide the eye.

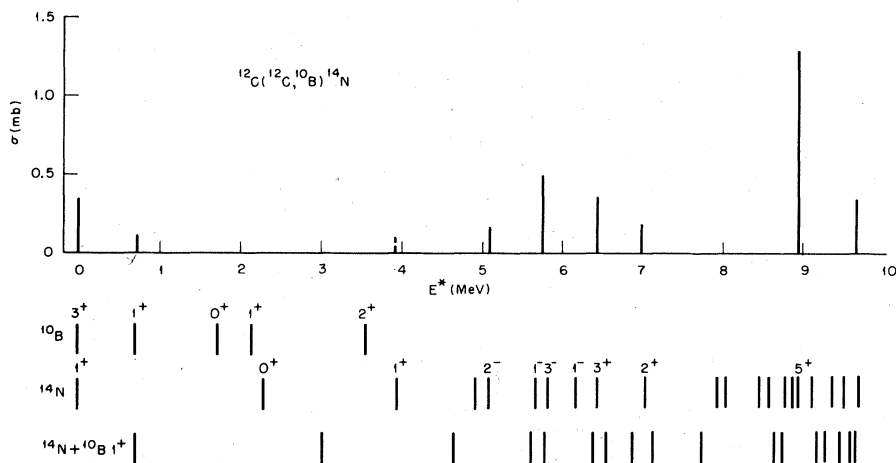


FIG. 6. Measured cross sections for  $np$  transfer reactions for  $^{12}\text{C} + ^{12}\text{C}$  at 93.8 MeV, where  $\sigma = 2\pi \int_{10}^{65} \sin \theta \sigma(\theta) d\theta$ .

TABLE I. Values of  $\sigma_{\text{int}}$  ( $10^\circ$ – $65^\circ$ ) for 93.8 MeV  $^{12}\text{C} + ^{12}\text{C}$  scattering<sup>a</sup> and most probable transfer reactions. The single-nucleon transfer reactions include all measured angular distributions for  $E^* < 5$  MeV and the  $pn$  transfer reactions include all observed peaks for  $E^* < 10$  MeV.

Reaction	$\sigma_{\text{int}}$ (mb)
Elastic scattering	37.5
Inelastic $2^+$ , single excitation	45.5
Inelastic $2^+$ , mutual excitation	14.0
Neutron transfer	2.02
Proton transfer	2.01
$pn$ transfer	3.49

<sup>a</sup> For the elastic and inelastic scattering, the scattered particle and the recoil nucleus are indistinguishable, and hence the measured cross sections include (equal) contributions from both. These cross sections should thus be divided by two for comparison with the transfer cross sections.

including  $np$  transfer in  $^{12}\text{C} + ^{12}\text{C}$  reactions. The model assumes that multiple nucleon transfer proceeds by transfer of a cluster of particles in relative  $S$  states with the center-of-mass of the cluster carrying all of the orbital angular momentum. In Fig. 8 we compare these predicted relative cross

sections with the integrated yields measured in the present work. While there are differences between the data and the model predictions, the agreement with the general trend of the data is sufficiently good to suggest the validity of the basic assumptions of the semiclassical model discussed in Ref. 23.

In the above we have referred to the two-nucleon transfer reactions measured in our work as “ $np$ ” transfer; but, except for comparison with predictions of the semiclassical model of Ref. 23, we have not considered the nature of the reaction. Anyas-Weiss *et al.*<sup>23</sup> considered two seemingly contradictory models. One is the transfer of a pair of correlated nucleons or cluster. The other model assumes that each of the transferred nucleons goes into a definite orbital  $nlj$ . At energies of  $\sim 10$  MeV/nucleon the velocity of the transferred nucleons at the surface of the target nucleus is matched to velocities in available orbits, and it is assumed that the two nucleons go into the maximum  $m$  states allowed by the Pauli principle and thus couple to the fully stretched state of maximum  $J$ . For states of high spin, the two descriptions are almost identical (Ref. 23). Both of these models assume that the transfer process is “single step.” Rae (Ref. 24) has pointed out that the

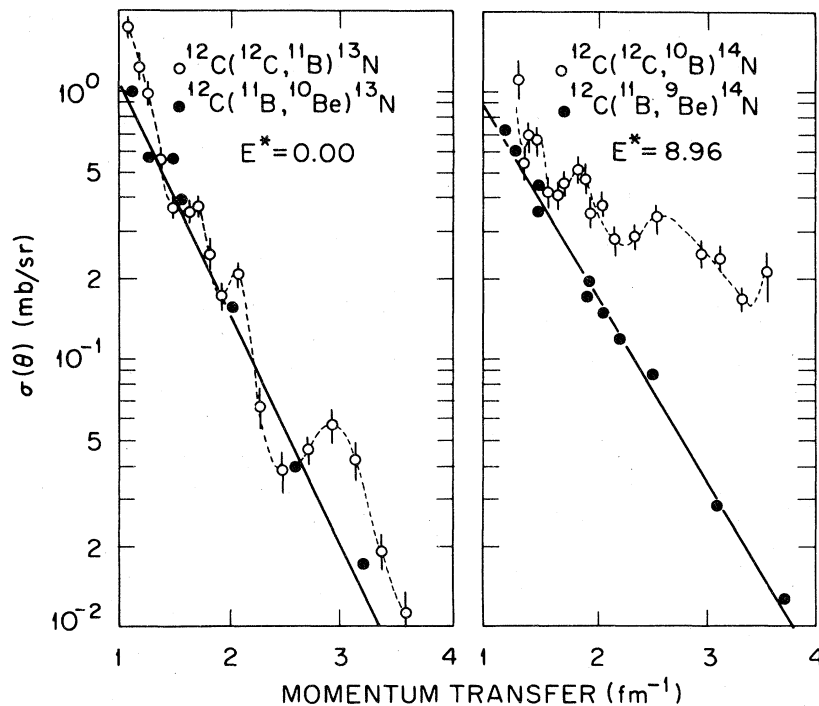


FIG. 7. Angular distributions for proton  $np$  transfers to  $^{12}\text{C}$  targets induced by 93.8 MeV  $^{12}\text{C}$  and 114 MeV  $^{11}\text{B}$  incident projectiles. The abscissa scale is in units of linear momentum transferred to the reaction product. The  $^{11}\text{B}$  data are from Ref. 3.

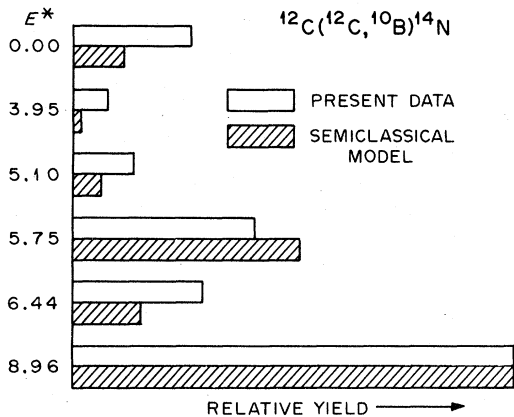


FIG. 8. Relative yields of  $np$  transfers in  $^{12}\text{C} + ^{12}\text{C}$  reactions. The present data are the total yields in the angular range  $10^\circ - 65^\circ$  and the calculated semiclassical model values are from Ref. 23. The two are normalized for the 8.96 MeV  $5^+$  level of  $^{14}\text{N}$ .

second model of two nucleons each going into definite orbits is more applicable to a sequential description than to a single step mechanism. When DWBA calculations for both the sequential model and the one-step model<sup>24</sup> are compared with data for a number of  $2n$  and  $2p$  transfer reactions, the sequential model yielded better agreement with experiment for some cases than did the one-step model.

For the present data, the following qualitative arguments suggest that sequential transfer is not an important component of  $^{12}\text{C}$  induced  $np$  transfer reactions on  $^{12}\text{C}$  targets. In Fig. 4 we see that neutron and proton transfers are very similar and that transfer to the  $p_{1/2}$  and  $d_{5/2}$  orbits occurs with comparable probability in single nucleon transfer. This implies that in "sequential" two-nucleon transfer the first transferred nucleon could be either a neutron or proton and would go into the  $p_{1/2}$  or  $d_{5/2}$  orbits with equal probability. In Fig. 6 we see that the  $5^+$  level at 8.96 MeV is the one most intensely excited in  $^{12}\text{C}(^{12}\text{C}, ^{10}\text{B})^{14}\text{N}$  reactions. The wave function for the 8.96 MeV  $5^+$  state of  $^{14}\text{N}$  contains a factor  $|\hat{d}_{5/2}^2\rangle|^{12}\text{C}0^+\rangle$ . Wave functions for levels such as the  $2^-$  at 5.11 MeV and the  $3^-$  at 6.44 MeV include the factor  $|\hat{p}_{1/2}\hat{d}_{5/2}\rangle|^{12}\text{C}0^+\rangle$ . We

see in Fig. 6 that the cross section for exciting the  $5^+$  level is approximately equal to the sum of those for the  $1^+$ ,  $2^-$ , and  $3^-$  levels. If the first nucleon in a sequential transfer goes into the  $p_{1/2}$  and  $d_{5/2}$  orbits with equal probability, it seems unlikely that the second nucleon of the  $n, p$  or  $p, n$  sequence would go predominantly into the  $d_{5/2}$  orbit so as to yield the relative cross sections observed. This qualitative argument does not include any coupling effects or the effect of  $Q$  values for the second step of the possible sequential transfer (i.e.,  $n, p$  and  $p, n$ ).

#### DWBA ANALYSIS

The assumption that the transfer reactions discussed above proceed through a one-step direct process was tested by comparing angular distributions for the stronger peaks observed in one-nucleon transfer with those predicted by distorted-wave-Born-approximation calculations. For these calculations the program LOLA,<sup>32</sup> which takes into account effects due to finite range and recoil, was used. The program was adapted<sup>34</sup> for the symmetric case of identical projectile and target. The nucleon (or cluster) is bound to the core in a Woods-Saxon potential with  $r_0 = 1.15$  and  $a_0 = 0.65$  fm in both bound states. The radius parameter, which is slightly smaller than the value of 1.25 which has often been used in similar calculations, was selected as the one that gives root-mean-square radii of the matter distribution most consistent with rms values from electron scattering data.<sup>35</sup> For the calculations with Woods-Saxon potentials, the same optical model parameters were used in the outgoing as in the incoming channels. Calculations using folding-model potentials were also performed, and for these calculations the potentials for each channel were computed separately.

The folding-model real potential that gave the best agreement with the elastic and inelastic scattering data (Ref. 21) was used for all reactions for which DWBA calculations were performed. The absorptive part of the potential had a Woods-Saxon form factor with the parameters listed in Table II. In the analyses of Ref. 21 the normalization

TABLE II. Optical model potentials used in the DWBA calculations. For calculations with potential A, a normalization of 1.12 was used for the real potential.

Potential	Form factor	$V$	$r_R$	$a_R$	$W_v$	$r_v$	$a_v$	Ref.
A	Folding model—real Woods-Saxon—imaginary				13.5	1.22	0.54	21
B	Woods-Saxon	81.1	1.02	0.68	66.0	1.19	0.38	23
C	Woods-Saxon	44.2	1.05	0.683	28.3	1.05	0.683	33

$N$  for the real potential was a parameter which varied with incident particle energy. For the 93.8 MeV DWBA calculations a value of  $N=1.12$  was used. For one case, however, the DWBA calculation was repeated with  $N=1.05$  with almost no effect on the predicted angular distribution, in marked contrast to the resulting effect on the elastic and inelastic scattering.

DWBA calculations with Woods-Saxon real potentials were also performed for the neutron transfer

reactions. Two potentials that were used are listed in Table II. Potential  $B$  was adopted as the preferred one for the DWBA calculations by Rae<sup>24</sup> for transfer reactions induced by  $^{12}\text{C}$  and  $^{16}\text{O}$  on  $^{12}\text{C}$  targets. Potential  $C$  was obtained in analysis of elastic scattering  $^{12}\text{C}+^{12}\text{C}$  data at 127 MeV.<sup>36</sup>

Figure 9 compares the measured angular distribution for neutron transfer to the ground state of  $^{13}\text{C}$  with the DWBA predictions for the three potentials that were used. All three calculated

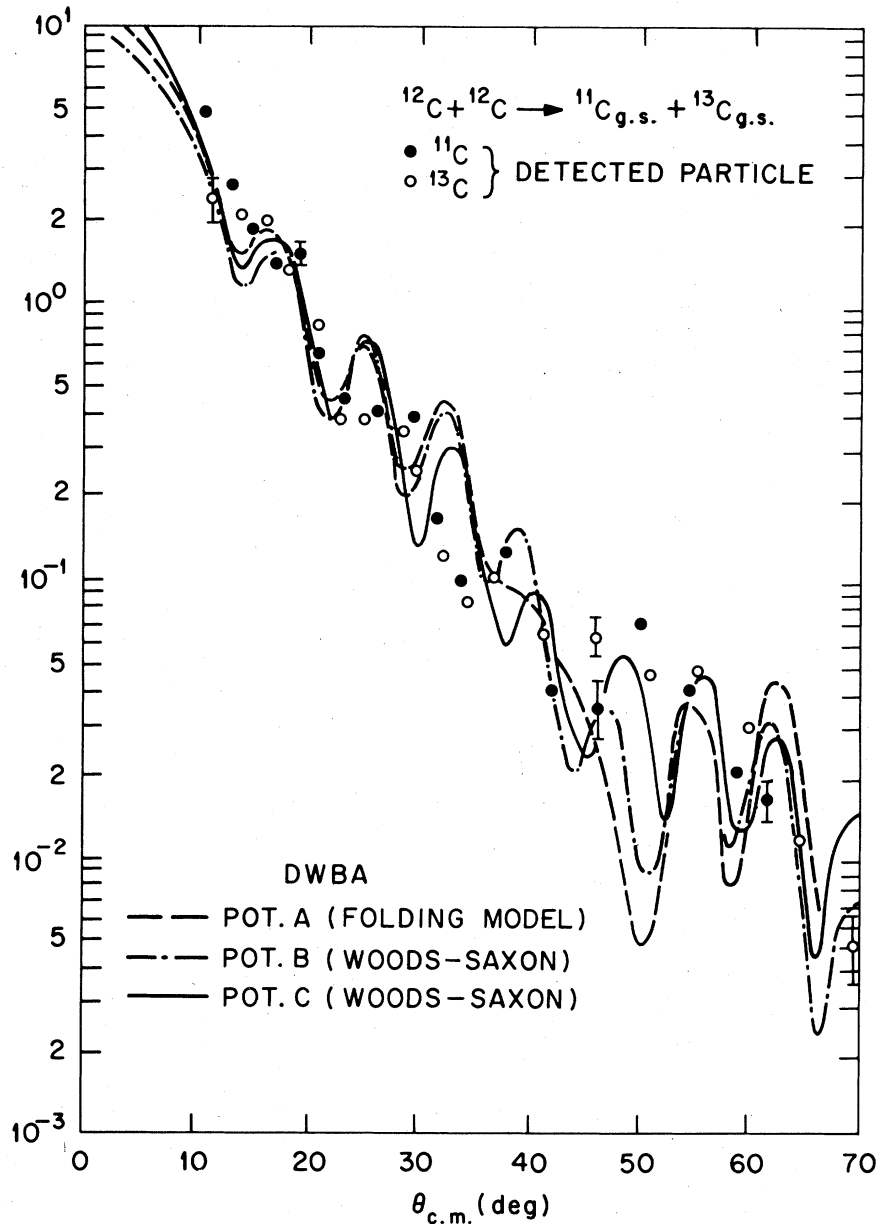


FIG. 9. Experimental and theoretical angular distributions for neutron transfer to ground states of  $^{11}\text{C}$  and  $^{13}\text{C}$ . Angular momentum transfers of  $L=1.2$  were used in the DWBA calculations. The potentials are described in Table II and the products of spectroscopic factors  $C_1^2 S_1 \times C_2^2 S_2$  are listed in Table III.

TABLE III. Spectroscopic factors.  $E^*$  is the excitation of  $B$  in the reaction  $A(a, b)B$ ;  $b$  is in the ground state for all of the DWBA calculations performed.

Reaction	$E^*$ (MeV)	Single particle orbitals		$l$ transfer	$C_1^2 S_1 \times C_2^2 S_2$	
		( $a, b$ )	( $A, B$ )		this work	other
$^{12}\text{C}(^{12}\text{C}, ^{11}\text{C})^{13}\text{C}$	0.00	$1p_{3/2}$	$1p_{1/2}$	1, 2	Pot. A 3.50	2.97 <sup>a</sup>
					Pot. B 3.00	1.74 <sup>b</sup>
					Pot. C 3.00	1.88 <sup>c</sup>
$^{12}\text{C}(^{12}\text{C}, ^{11}\text{C})^{13}\text{C}$	3.85	$1p_{3/2}$	$1d_{5/2}$	1, 2, 3	Pot. A 1.42	1.62 <sup>a</sup>
					Pot. C 1.17	0.71 <sup>c</sup>
$^{12}\text{C}(^{12}\text{C}, ^{11}\text{B})^{13}\text{N}$	0.00	$1p_{3/2}$	$1p_{1/2}$	1, 2	Pot. A 3.50	2.50 <sup>a</sup>
						1.88 <sup>c</sup>

<sup>a</sup> Reference 24 (obtained from analysis of data).

<sup>b</sup> Reference 37 (theoretical value).

<sup>c</sup> Reference 23 (theoretical value).

angular distributions follow the trend of the data over the full angular range although none reproduces the details. At angles forward of  $30^\circ$  there is no preference for any of the potentials. In the

$30^\circ$ – $50^\circ$  region, the data exhibit two minima as do the DWBA predictions with the two Woods-Saxon potentials,  $B$  and  $C$ . The prediction with the folding-model potential ( $A$ ), however, shows only a

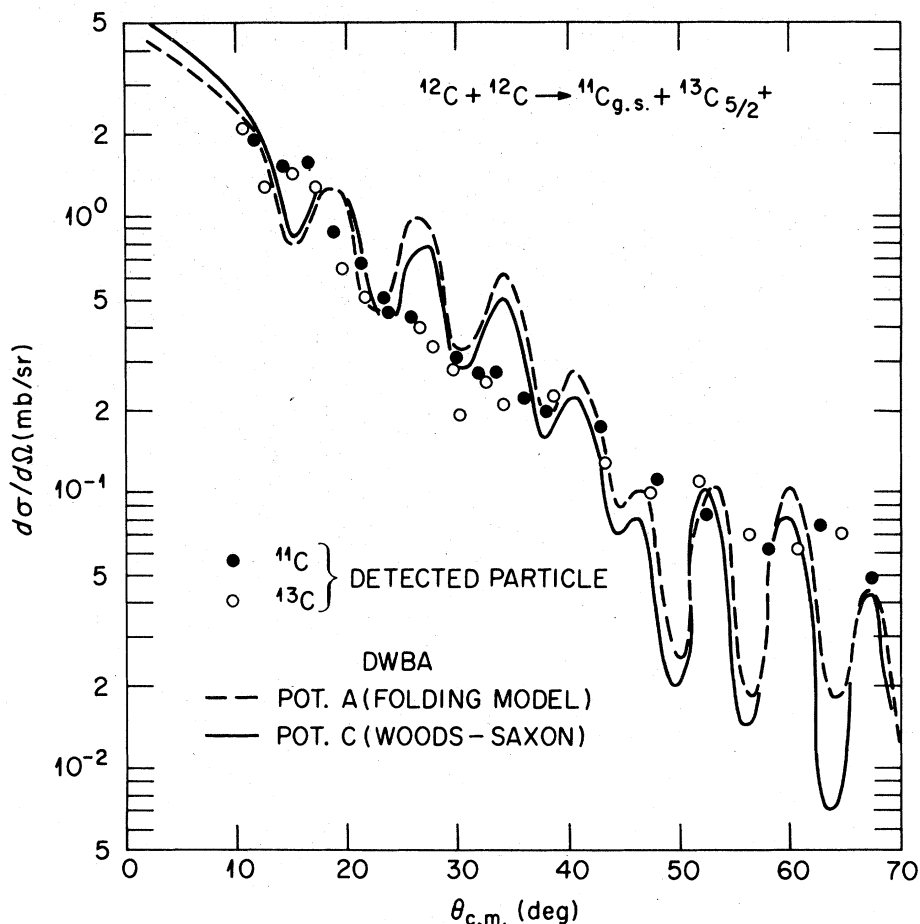


FIG. 10. Experimental and theoretical angular distributions for neutron transfer to the ground state of  $^{11}\text{C}$  and the  $3.85\text{ MeV } \frac{5}{2}^+$  state of  $^{13}\text{C}$ . Angular momentum transfers of  $L+1, 2, 3$  were used in the DWBA calculations. The potentials are described in Table II and the products of spectroscopic factors  $C_1^2 S_1 \times C_2^2 S_2$  are listed in Table III.

hint of one minimum ( $\sim 38^\circ$ ) in this angular region. Better overall agreement with the data is apparently obtained using the Woods-Saxon potentials rather than the folding-model potential.

The products of the spectroscopic factors ( $C^2S$ ) obtained by adjusting the DWBA predictions to the data are listed in Table III and compared with results of other work. The values obtained with the two Woods-Saxon potentials are equal and agree with the value obtained from analysis of 114 MeV data<sup>24</sup> using potential *B*. The spectroscopic factors obtained in both the present work and that of Ref. 24 are larger than the calculated values from Refs. 24 and 27.

Figure 10 compares the measured angular distribution for neutron transfer to the  $\frac{5}{2}^+$  level of  $^{13}\text{C}$  with DWBA predictions for the folding-model potential and one of the Woods-Saxon potentials.

The general trend of the data is followed by the DWBA predictions, but the predictions show much more pronounced oscillations. The data in Fig. 10 do not discriminate between the folding-model and Woods-Saxon potentials as did the data in Fig. 9 for ground state. The products of spectroscopic factors are listed in Table III and compared with results of other work.

In Fig. 11 we compare the measured angular distribution for proton transfer to the ground state of  $^{13}\text{N}$  with the DWBA prediction for potential *A*. The prediction was normalized for the same product of spectroscopic factors as for the neutron transfer case with potential *A* (Fig. 9). The integrated yields for proton and neutron transfer are equal for both the ground and  $\frac{5}{2}^+$  states (Fig. 4). There are some differences in the calculated angular distributions for neutron and proton transfer

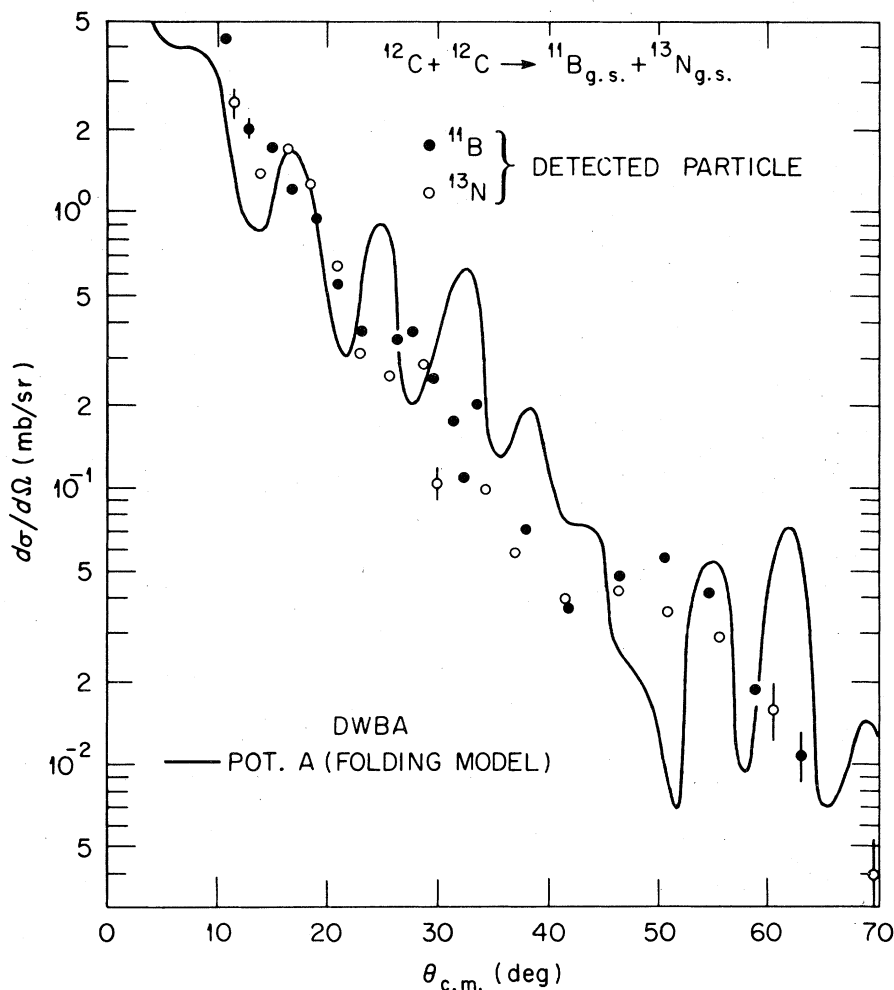


FIG. 11. Experimental and theoretical angular distributions for proton transfer to ground states of  $^{11}\text{B}$  and  $^{13}\text{N}$ . Angular momentum transfers of  $L=1, 2$  were used in the DWBA calculation. The potential is described in Table II and the product of spectroscopic factors  $C_1^2S_1 \times C_2^2S_2$  is listed in Table III.

to the ground states. While the  $Q$  values differ by only 0.24 MeV, there are larger differences ( $\sim 3$  MeV) in the respective separation energies for the bound states which are principally due to Coulomb effects. It thus appears that the DWBA calculations are sensitive to these differences. We did not perform DWBA calculations for proton transfer to the  $\frac{5}{2}^+$  state of  $^{13}\text{N}$  since excited states of  $^{13}\text{N}$  are unbound to particle emission.

#### SUMMARY AND CONCLUSIONS

The data presented above constitute rather complete angular distributions of the most intense one- and two-nucleon transfers in 93.8 MeV  $^{12}\text{C} + ^{12}\text{C}$  reactions. The transfer reactions are selective in that only a few of the available states are strongly excited; the cross sections for these are small compared to those for elastic and inelastic scattering. Over the angular range of the data, the sum of the integrated cross sections for all of the measured one- and two-nucleon transfers is comparable to that of the mutual excitation of the

$2^+$  (4.44 MeV) level in  $^{12}\text{C}$ .

It is unlikely that double transfer contributions to elastic and inelastic scattering can be calculated accurately, because such a calculation would have to take into account many transfer reactions, each of which is small as can be seen from the results discussed above. It appears that double transfer effects, if they are present, are adequately mocked up by the use of a complex potential.

There are differences, revealed by qualitative comparisons, between  $^{12}\text{C}$  induced transfer reactions and those induced by  $^{11}\text{B}$ ,  $^{14}\text{N}$ , and  $^{16}\text{O}$  on  $^{12}\text{C}$  targets. These may be caused by individual differences in  $Q$  value, but detailed DWBA analysis of all of these reactions would be needed to assess the significance of these differences. DWBA analyses do account for the shapes of one-nucleon transfer angular distributions and yield reasonable spectroscopic factors.

Oak Ridge National Laboratory is operated by Union Carbide Corporation for the Department of Energy.

<sup>1</sup>G. C. Morrison, Phys. Rev. Lett. **5**, 565 (1960).

<sup>2</sup>D. A. Bromley, K. Nagatani, L. C. Northcliffe, R. Ollerhead, and A. R. Quinton, in *Proceedings of the Rutherford Jubilee International Conference, Manchester, 1961*, edited by J. B. Birks (Heywood, London, 1962), p. 597.

<sup>3</sup>M. W. Sachs, C. Chasman, and D. A. Bromley, Phys. Rev. **139**, B92 (1965).

<sup>4</sup>J. Birnbaum, J. C. Overley, and D. A. Bromley, Phys. Rev. **157**, 787 (1967).

<sup>5</sup>J. E. Poth, J. C. Overley, and D. A. Bromley, Phys. Rev. **164**, 1295 (1967).

<sup>6</sup>H. J. Körner, G. C. Morrison, L. R. Greenwood, and R. H. Siemssen, Phys. Rev. **C 7**, 107 (1973).

<sup>7</sup>P. D. Bond, J. D. Garrett, O. Hansen, S. Kahana, M. J. LeVine, and A. Z. Schwarzschild, Phys. Lett. **47B**, 231 (1973).

<sup>8</sup>M. J. Schneider, C. Chasman, E. H. Auerbach, A. J. Baltz, and S. Kahana, Phys. Rev. Lett. **31**, 320 (1973).

<sup>9</sup>C. Chasman, S. Kahana, and M. J. Schneider, Phys. Rev. Lett. **31**, 1074 (1973).

<sup>10</sup>P. R. Christensen, O. Hansen, J. S. Larsen, D. Sinclair, and F. Videbaek, Phys. Lett. **45B**, 107 (1973).

<sup>11</sup>J. B. Ball, O. Hansen, J. S. Larsen, D. Sinclair, and F. Videbaek, Phys. Lett. **49B**, 348 (1974).

<sup>12</sup>J. Paschopoulos, P. S. Fisher, N. A. Jelley, S. Kahana, A. A. Pilt, W. D. M. Rae, and D. Sinclair, Nucl. Phys. **A252**, 173 (1975).

<sup>13</sup>W. J. Swiatecki, J. Phys. (Paris) **33C**, 5 (1972).

<sup>14</sup>M. Blann and F. Plasil, Phys. Rev. Lett. **29**, 303 (1972).

<sup>15</sup>D. M. Brink, Phys. Lett. **40B**, 37 (1972).

<sup>16</sup>S. Raman, C. B. Fulmer, M. L. Halbert, M. J. Saltmarsh, A. H. Snell, and P. H. Stelson, in *Proceedings of the International Conference on Reactions between Complex Nuclei, Nashville, Tennessee, 1974*, edited by R. L. Robinson, F. K. McGowan, J. B. Ball, and

J. H. Hamilton (North-Holland, Amsterdam/American Elsevier, New York, 1974), Vol. I, p. 2.

<sup>17</sup>R. G. Stokstad, C. B. Fulmer, M. L. Halbert, S. Raman, D. C. Hensley, A. H. Snell, and P. H. Stelson, Physics Division Annual Progress Report, 1974, Report No. ORNL-5025 (unpublished), p. 46.

<sup>18</sup>R. M. Wieland, C. B. Fulmer, D. C. Hensley, S. Raman, L. D. Rickertsen, A. H. Snell, P. H. Stelson, R. G. Stokstad, and G. R. Satchler, Physics Division Annual Progress Report, 1975, Report No. ORNL-5137 (unpublished), p. 42.

<sup>19</sup>R. M. Wieland, R. G. Stokstad, G. R. Satchler, and L. D. Rickertsen, Phys. Rev. Lett. **37**, 1458 (1976).

<sup>20</sup>R. G. Stokstad, R. M. Wieland, C. B. Fulmer, D. C. Hensley, S. Raman, A. H. Snell, P. H. Stelson, Oak Ridge National Laboratory Report No. ORNL/TM 5235, 1977 (unpublished).

<sup>21</sup>R. G. Stokstad *et al.*, preceding paper, Phys. Rev. **C 20**, 665 (1979).

<sup>22</sup>D. K. Scott, P. M. Hudson, P. S. Fisher, C. U. Cardinal, N. Anyas-Weiss, A. D. Panagiotou, and P. J. Ellis, Phys. Rev. Lett. **28**, 1659 (1972).

<sup>23</sup>N. Anyas-Weiss, J. C. Cornell, P. S. Fisher, P. N. Hudson, A. Menchaca-Rocha, D. J. Millener, A. D. Panagiotou, D. K. Scott, D. Strottman, D. M. Brink, B. Buck, P. J. Ellis, and T. England, Phys. Rep. **12C**, 201 (1974).

<sup>24</sup>W. D. M. Rae, thesis, Oxford University, 1976 (unpublished).

<sup>25</sup>S. Barshay and G. M. Temmer, Phys. Rev. Lett. **12**, 728 (1964).

<sup>26</sup>L. D. Rickertsen, Oak Ridge National Laboratory Report No. ORNL-5025, 1975 (unpublished), p. 17.

<sup>27</sup>P. Schumacher, N. Ueta, H. H. Kuhm, K. I. Kubo, and W. J. Kleges, Nucl. Phys. **A212**, 573 (1973).

<sup>28</sup>W. Von Oertzen, M. Liu, C. Caverzasio, J. C. Jacmart,

- F. Pougheon, M. Riou, J. C. Roynette, and C. Stephen, Nucl. Phys. A143, 34 (1970).
- <sup>29</sup>K. G. Nair, H. Voit, C. W. Towsley, M. Hamm, J. D. Bronson, and K. Nagatani, Phys. Rev. C 12, 1575 (1975).
- <sup>30</sup>L. R. Dodd and K. R. Greider, Phys. Rev. Lett. 14, 959 (1965).
- <sup>31</sup>R. M. DeVries and K. I. Kubo, Phys. Rev. Lett. 30, 325 (1973).
- <sup>32</sup>R. M. DeVries, Phys. Rev. C 8, 951 (1973).
- <sup>33</sup>R. M. DeVries, M. S. Zisman, J. G. Cramer, and K. L. Liu, Phys. Rev. Lett. 32, 680 (1974).
- <sup>34</sup>L. W. Owen and L. D. Rickertsen (unpublished).
- <sup>35</sup>C. W. DeJaeger, H. DeVries, and C. DeVries, At. Data Nucl. Data Tables 14, 479 (1974).
- <sup>36</sup>R. H. Bassel, G. R. Satchler, and R. M. Drisko, Nucl. Phys. 89, 419 (1966).
- <sup>37</sup>S. Cohen and D. Kurath, Nucl. Phys. A101, 1 (1967).